Communication

Label-Free, Portable, and Color-Indicating Cholesteric Liquid Crystal Test Kit for Acute Myocardial Infarction by Spectral Analysis and Naked-Eye Observation

Fu-Lun Chen [1,2,†], Li-Dan Shang [3], Yen-Chung Lin [2,4,5,†], Bo-Yen Chang [6,†] and Yu-Cheng Hsiao [7,8,9,*]

1. Department of Internal Medicine, Division of Infectious Diseases, Wan Fang Hospital, Taipei Medical University, No.111, Sec. 3, Xinglong Rd., Wenshan Dist., Taipei 11600, Taiwan
2. Department of Internal Medicine, School of Medicine, College of Medicine, Taipei Medical University, 250 Wuxing St., Taipei 11031, Taiwan
3. Department of Geography and Planning, University of Liverpool, Liverpool L69 3BX, UK
4. Department of Internal Medicine, Division of Nephrology, Taipei Medical University Hospital, 252 Wuxing St., Taipei 110, Taiwan
5. TMU Research Center of Urology and Kidney (TMU-RCUK), Taipei Medical University, Taipei 110, Taiwan
6. Department of Biomedical Engineering, Taipei Medical University, Taipei 11031, Taiwan
7. Graduate Institute of Biomedical Optomechatronics, College of Biomedical Engineering, Taipei 11031, Taiwan
8. International PhD Program for Biomedical Engineering, Taipei Medical University, Taipei 11031, Taiwan
9. Cell Physiology and Molecular Image Research Center, Wan Fang Hospital, Taipei Medical University, Taipei 11031, Taiwan
* Correspondence: ychsiao@tmu.edu.tw
† These authors contributed equally to this work.

Abstract: The early diagnosis of acute myocardial infarction is difficult in patients with nondiagnostic characteristics. Acute myocardial infarction with chest pain is associated with increased mortality. This study developed a portable test kit based on cholesteric liquid crystals (CLCs) for the rapid detection of AMI through eye observation at home. The test kit was established on dimethyloctadecyl[3-(trimethoxysilyl)propyl]ammonium chloride-coated substrates covered by a CLC-binding antibody. Cardiac troponin I (cTnI) is a major biomarker of myocardial cellular injury in human blood. The data showed that the concentration of cTnI was related to light transmittance in a positive way. The proposed CLC test kit can be operated with a smartphone; therefore, it has high potential for use as a point-of-care device for home testing. Moreover, the CLC test kit is an effective and innovative device for the rapid testing of acute myocardial infarction-related diseases through eye observation, spectrometer, or even smartphone applications.

Keywords: acute myocardial infarction rapid test; cholesteric liquid crystal; cardiac troponin I (cTnI)

1. Introduction

An early acute myocardial infarction (AMI) diagnosis can be difficult for patients with nondiagnostic features. Cardiac troponin I (cTnI) is the inhibitory subunit of the troponin complex and can inhibit the binding of actin and myosin; cTnI plays a major role in AMI [1–3]. The studies have shown that cTnI concentration increases rapidly during the early stage of AMI [4,5]. Furthermore, cTnI is highly specific to cardiomyocytes but not to skeletal muscles [6–8]. The cTnI has a sensitivity and specificity of 96% and 97% in AMI diagnosis, respectively [9–11]. In addition, cTnI serves as a major serum biomarker of injury for myocardial cellular, and it affords the advantage of clear diagnostic thresholds and rapid detection, which are crucial for the assessment of AMI patients with myocardial cell injury [12,13]. The cTnI concentrations are associated with the extent of the cardiac injury; the high cTnI concentrations (100 μg/mL) indicate myocardial infarction [13,14]. Therefore, quick cTnI quantification and detection are crucial for the assessment of cardiac injury, thus necessitating the development of a label-free, rapid, and low-cost cTnI detection

bio-device. Several methods are available for measuring cTnI, including ELISA [15,16], fluorescence immunoassay [17–19], colorimetric [20], electrochemical [21], paramagnetic [22], and surface plasmon resonance [23] methods, etc. However, when compared to liquid crystal (LC) biosensors, these approaches are disadvantaged due to sophisticated equipment and time-consuming processes. Accordingly, developing a fast, label-free, sensitive, and low-cost device for detecting the cTnI level is imperative.

Recent studies have shown that LC biosensors can successfully diagnose diseases [24–32]. Biomolecules can redirect LC molecules, causing changes in the light signal's intensity [33]. The redirected LC molecules cause a sensitive response to changes in the optical signal. The studies have integrated LC with microfluidic detection of bovine serum albumin [34,35]. Additionally, cholesteric liquid crystals (CLCs) have distinct viewing angles when compared to nematic LCs: bistability, Bragg reflection, and flexibility [36–39]. In 2015, the CLC high-sensitivity biological sensor (limit of detection = 1 fg/mL) was developed for detecting bovine serum albumin [40].

The present paper invented the color-specific CLC test kit for rapidly testing AMI through eye observation. The study used a pair of substrates coated with a cTnI antigen/peptide and the CLCs to perform an assay. The proposed CLC test kit is different from previous normal biosensors. The level of cTnI antigen/peptide could be observed and measured with the naked eye. The alignment layers of N,N-dimethyl-n-octadecyl-3-aminopropyltrimethoxysilyl chloride (DMOAP) were employed to sense the cTnI levels [41]. The schematic of the proposed CLC test kit is illustrated in Figure 1. According to our review of the literature, this is the paper to use color CLC biochips as a new medical approach to identify the pathological severity of AMI-related diseases through early detection of cTnI. The innovation of the study is that it presents the bio-device for rapid AMI testing at home with point-of-care.
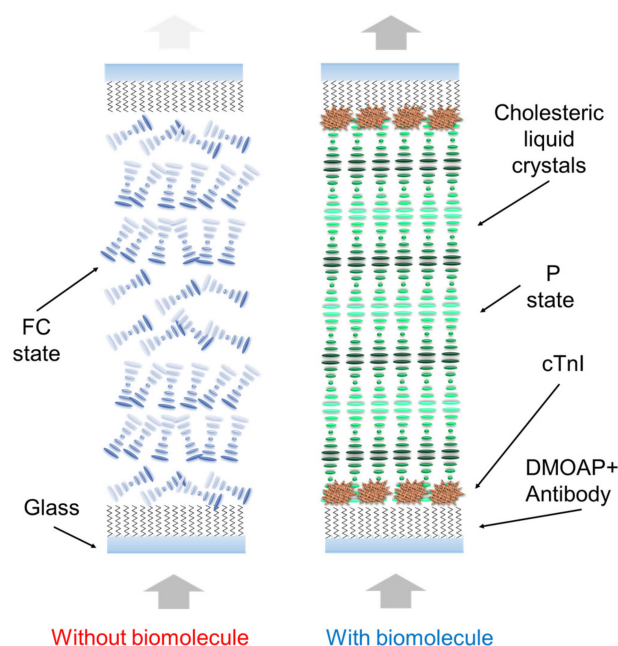

Figure 1. Schematic of the CLC test kit for rapid AMI testing. DMOAP enables CLC molecules to be vertically aligned. Schematic of the cTnI and peptide immunocomplex on the glass substrate.

2. Materials and Methods

The mechanism of the proposed novel CLC test kit is displayed in Figure 2. The test kit executes optical detection using cross-polarized microscopy through a spectrometer. The test kit estimates the concentration of cTnI in a sample according to the intensity of light signals. DMOAP—serving as the alignment layer in the sensor—has a long carbon chain that can align CLC molecules vertically. The nematic LC E7 and chiral dopant R5011 were used in this study's experiment. To enable DMOAP to respond to cTnI, it is covered

by the additional JP5-19H peptide as an antibody layer. Specific immune complexes crowd out and disrupt the arrangement of CLC molecules. The adsorption of an immune complex on a substrate engenders a bright light signal owing to the planar state of the CLC test kit (Figure 1, right panel). Because the light intensity is positively related to the cTnI concentration, the presence of cTnI can easily be recognized. Accordingly, the biosensor quantifies the light intensity signal passing through the CLC molecule, thus enabling the estimation of the level of cTnI in unknown samples.
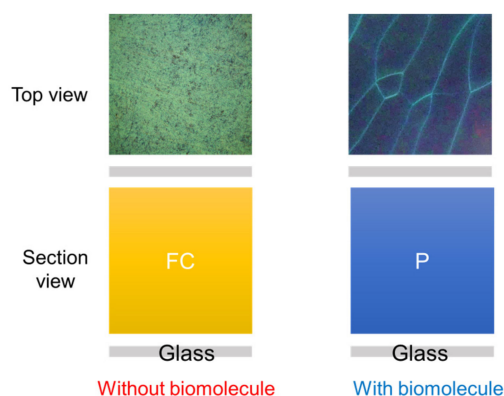

Figure 2. In the presence of abundant biomolecules on the DMOAP substrate, the configuration changes from a predominant reflection mode to a predominant transmission mode.

Step 1. Coating the alignment layer:

Glass substrates were used in the experiments. The substrates were cleaned with deionized water (DI water) and vibrated ultrasonically twice in the container for 15 min in order to eliminate dust. Subsequently, wash with DI water (50 mL) for half a day, followed by DECON-90 with 2.5 mL. The substrates were rinsed with DI water and vibrated in the ultrasonic shaker for 15 min again. We chose the DMOAP as the alignment layer. DMOAP is $C_{18}H_{37}$, which arranges CLC molecules vertically (Figure 1). The cleaned glass was nicely stacked in the container and completely immersed in the DMOAP with 1 wt% Subsequently, a solution was agitated on an ultrasonic shaker for several minutes and rinsed with DI water to remove any excess DMOAP.

Step 2. Producing the immunoassay layer:

Single biomolecular layer: According to the detection principle for CLC test kits, a single biomolecular layer should be used to assess different concentrations of cTnI samples. As a result, different levels of cTnI were produced using DI water solvent. To obtain the LOD, we first employed a broad concentration range (i.e., 0.01, 0.1, 1, 10, and 100 g/μL) and lowered the concentration range gradually.

Preparing double immunoassay layers: A double-layer immunoassay was used to examine the effect of the brightness on the different levels of cTnI and peptides, measure optical intensity, and confirm the brightness-concentration association. We found the optimal peptide concentration for cTnI detection and measured the brightness after validating the link between peptide and cTnI levels. The required preparation steps are outlined below.

The peptide drops (0.5 μL) at different concentrations on the alignment layer. After the lower substrate had dried, cTnI with 40 μL was dropped on the first peptide layer and covered with another clean substrate to ensure that cTnI was equally distributed on the layer of peptide. We allowed 1 h for the immune reaction between the applied cTnI and the peptide. Next, the upper glass substrate was removed, and then the lower glass substrate was dried.

Step 3. Making the CLC layer:

The two thin glass substrates with the alignment DMOAP coating were used to make a CLC cell. The CLC E7 and the chiral dopant R5011 were filled between the two basic glass substrates. Subsequently, CLCs were distributed in the cell uniformly through capillary action. Finally, we seal four edges of the substrate using AB glue.

3. Results

In order to display the characteristics of the CLC test kit that can be observed by the naked eye and smartphones. Figure 3 depicts polarized optical images captured by the proposed CLC test kit—operated by a smartphone—under cross-polarization. The optical texture of the CLC test kit under various concentrations of cTnI is displayed in Figure 3. We observed that the optical brightness increased with the cTnI concentration. Moreover, we observed that the CLC molecules were randomly in a focal conic (FC) state around the two substrates. When cTnI was immobilized on the coated substrate, the CLC molecules were noted to be completely in a planar (P) state. Light passing through the CLC material was scattered by some of the CLC molecules in the FC state. However, when cTnI was immobilized, the capacity of DMOAP to maintain the vertical alignment of the molecules was reduced (Figure 2). As the cTnI concentration increased, the CLC molecules switched from the FC state to the P state. Finally, the optical intensity of the CLC molecules in the P state increased (Figure 3). The optical texture of four CLC test kits under various concentrations of BSA is illustrated in Figure 3. It is worth noting that the chiral dopant material R5011 used in this study is temperature-independent [20]. Therefore, CLC test kits can be used conveniently and consistently at a wide range of room temperatures in different countries. In addition to using POM, CLC can be directly observed by naked eyes from the change in color [40]. In order to be able to more accurately determine the concentration of the cTnI, we evaluated light intensity using the spectrometer with a fiber-based design and microscopy with cross-polarizers, a technique known as micro-reflective fiberoptic spectrophotometry (MRFS). We used a white LED light source. After the light had penetrated through the microscopic system, we measured cTnI concentrations on the basis of the intensity of the light (Figure 4). Polarized optical images of the CLC test kit were captured after the cTnI peptide interacted with cTnI of various concentrations under cross-polarization. The brightness level increased with the cTnI concentration under cross-polarization. The transmission spectra of the CLC test kit under 0–1 mg/mL of cTnI are presented in Figure 4. Results showed an LOD of 1 ng/mL for cTnI. Furthermore, it was revealed that the concentrations of cTnI were significantly associated with the intensities of the CLC test kit. We determined the detection mechanism and performance of the CLC test kit by using MRFS spectra. The transmittance spectra differed for the various concentrations of cTnI (0 µg/mL, 1 ng/mL, 1 µg/mL, and 1 mg/mL). We used a chromophore to measure the transmittance of the CLC test kit, with the minimum transmittance being observed at 500 nm due to the selective reflection of the CLCs (Figure 4). We captured the minimum intensity of light penetrating different concentrations of cTnI were quantified at a wavelength of 500 nm (Figure 5). The results show that the light penetrating the system at 500 nm is positively linearly related to the concentration of cTnI. It is worth noting that the penetration of the CLC chip will decrease after one hour, so the observation time must be completed within one hour.
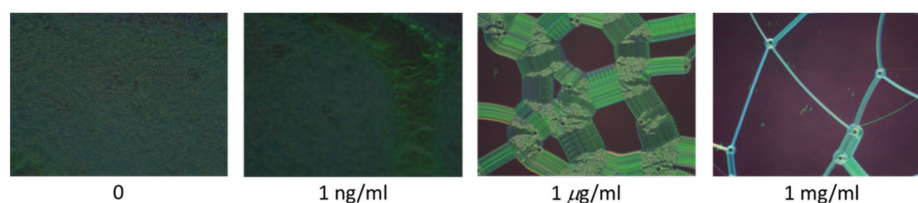

0	1 ng/ml	1 µg/ml	1 mg/ml

Figure 3. Polarized optical microscopic images captured by the CLC test kit operated by a smartphone under various concentrations of cTnI (0–1 mg/mL) immobilized on DMOAP-coated glass.

To bind the cTnI, we add another peptide layer. The intensity of transmitted light was then assessed at various peptide and cTnI concentrations, as shown in Figure 6, where the *x*-axis represents the level of peptide or anti-cTnI and the *y*-axis represents the optical intensity. The data show that the optimal peptide concentration for cTnI detection was 10 µg/mL. When the peptide concentration was excessively high at 20 µg/mL and

30 µg/mL, the peptide severely interfered with the CLC molecule. In addition, even when the cTnI concentration was zero, the transmittance was high. By contrast, when the peptide or anti-cTnI concentration was excessively lower than 20 µg/mL, the reorientation of the CLCs was not affected by cTnI. Accordingly, we could not detect the different concentrations of cTnI owing to the lack of a notable difference in brightness. When samples containing the peptide were filled between the double immunoassay layers, the disturbance power of the LC molecules increased. The LOD of cTnI was determined to be lower in the double immune layer than that in the single layer. Accordingly, the LC biosensor for rapid myocardial infarction testing has favorable selectivity between cTnI and biomolecules.
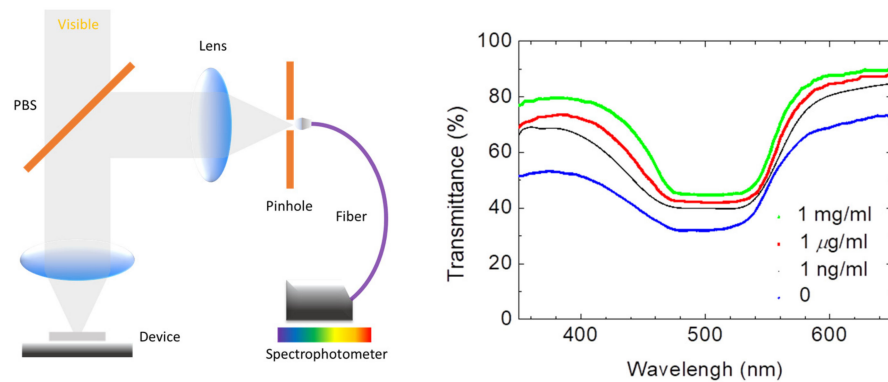

Figure 4. The schematic diagram of MRFS system and the spectra of the CLC test kit under 0–1 mg/mL of cTnI.
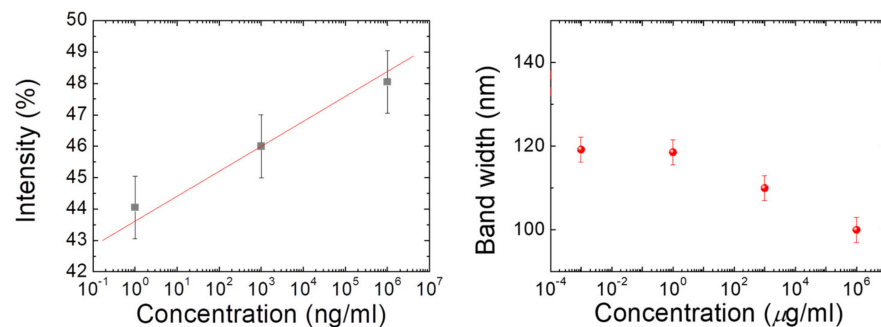

Figure 5. Linear correlation (determination coefficient $R^2 \geq 0.93$) obtained using 0–1 mg/mL of cTnI.
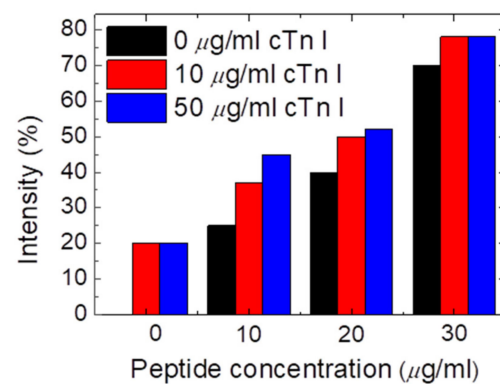

Figure 6. Intensity of an immunoassay CLC chip immobilized with peptide (concentration range from 0 to 30 µg/mL) and cTnI (concentration range from 0 to 50 µg/mL).

After identifying the optimal peptide concentration with 10 µg/mL prepared for cTnI detection, we employed it to assess the efficiency of the proposed CLC test kit in detecting different amounts of cTnI with 0–50 µg/mL. In addition, the test shows that the data was

applied to construct a calibration curve, as indicated in Figure 7. The data revealed that the cTnI concentrations were positively and linearly correlated with the optical intensity. Hence, the results indicate that cTnI concentrations in samples can be easily estimated using linear interpolation, as long as the concentration is within LOD. Furthermore, we established that the observed cTnI was 0–50 μg/mL (optimal peptide concentration: 10 μg/mL), with a 50 μg/mL exhibiting the brightness gain. Note that the reflection band of traditional CLC is very temperature-sensitive, but according to different chiral dopants, this conclusion has changed. Figure 8 shows the E7 doping with R5011, which is quite insensitive to temperature. In addition, the selectivity tests in cTnI are also shown in Figure 8.
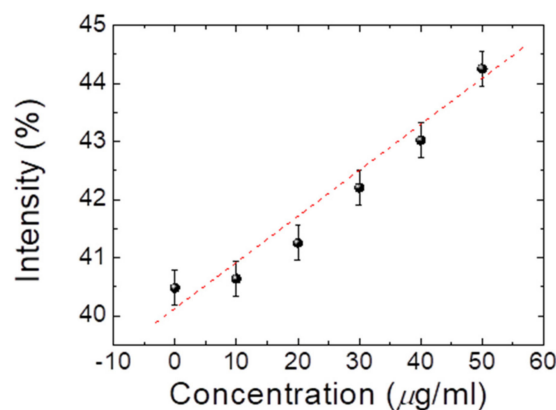

Figure 7. Correlation of light intensity with various cTnI concentrations in CLC biosensing chips with 10 μg/mL of peptide.
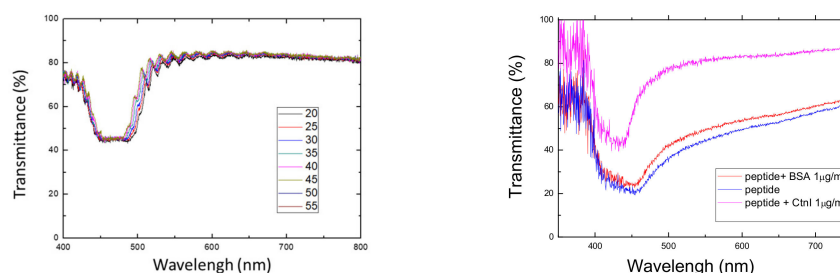

Figure 8. The spectra of the CLC test kit under different temperatures (left) and peptides with different biomolecules (right).

4. Conclusions

This study is the first to present a CLC test kit for rapid AMI testing. The CLC test kit can detect monolayer cTnI samples and shows a LOD of 1 ng/mL for cTnI. Under crossed polarized microscopy, the cTnI level was positively linked with transmitted intensity. The photon has the maximum cyan reflectance at a wavelength of approximately 500 nm, as revealed by a spectrometer. We also determined that the optimal peptide concentration for binding cTnI between immunoassay layers was 10 μg/mL. In addition, we observed a positive relation between the concentration of cTnI and the transmittance of light. The LOD of cTnI immunoassay double layers, on the other hand, was less than 10 μg/mL. Furthermore, when observed using a smartphone camera, the optical intensity showed the same clear pattern of positive correlation as that observed with the naked eye. These results corroborate the potential of successfully testing for AMI by measuring the concentrations of cTnI. Accordingly, the proposed test kit has potential for use as a point-of-care test kit operated with a smartphone for home or clinical testing of AMI. Nematic liquid crystals provide an efficient method for rapid AMI testing using cross-polarized microscopes, smartphones, spectrometers, or the naked eye.

References

1. Westfall, M.; Rust, E.; Metzger, J.; Westfall, M.V.; Rust, E.M.; Metzger, J.M. Slow skeletal troponin I gene transfer, expression, and myofilament incorporation enhances adult cardiac myocyte contractile function. *Proc. Natl. Acad. Sci. USA* **1997**, *94*, 5444–5449. [CrossRef] [PubMed]
2. Ramirez-Correa, G.A.; Murphy, A.M. Is phospholamban or troponin I the "prima donna" in beta-adrenergic induced lusitropy? *Circ. Res.* **2007**, *101*, 326–327. [CrossRef] [PubMed]
3. Eggers, K.; Lind, L.; Ahlström, H.; Bjerner, T.; Barbier, C.E.; Larsson, A.; Venge, P.; Lindahl, B. Prevalence and pathophysiological mechanisms of elevated cardiac troponin I levels in a population-based sample of elderly subjects. *Eur. Heart J.* **2008**, *29*, 2252–2258. [CrossRef] [PubMed]
4. Boeddinghaus, J.; Twerenbold, R.; Nestelberger, T.; Badertscher, P.; Wildi, K.; Puelacher, C.; de Lavallaz, J.F.; Keser, E.; Giménez, M.R.; Wussler, D. Clinical validation of a novel high-sensitivity cardiac troponin I assay for early diagnosis of acute myocardial infarction. *Clin. Chem.* **2018**, *64*, 1347–1360. [CrossRef]
5. Lippi, G.; Favaloro, E.; Kavsak, P. *Measurement of High-Sensitivity Cardiac Troponin in Pulmonary Embolism: Useful Test or a Clinical Distraction, Seminars in Thrombosis and Hemostasis*; Thieme Medical Publishers: New York, NY, USA, 2019; pp. 784–792.
6. Kim, L.; Martinez, E.; Faraday, N.; Dorman, T.; Fleisher, L.; Perler, B.; Williams, G.; Chan, D.; Pronovost, P. Cardiac troponin I predicts short-term mortality in vascular surgery patients. *Circulation* **2002**, *106*, 2366–2371. [CrossRef] [PubMed]
7. Kavsak, P.; MacRae, A.; Yerna, M.; Jaffe, A. Analytic and clinical utility of a next-generation, highly sensitive cardiac troponin I assay for early detection of myocardial injury. *Clin. Chem.* **2009**, *55*, 573–577. [CrossRef] [PubMed]
8. Melanson, S.; Morrow, D.; Jarolim, P. Earlier detection of myocardial injury in a preliminary evaluation using a new troponin I assay with improved sensitivity. *Am. J. Clin. Pathol.* **2007**, *128*, 282–286. [CrossRef]
9. Labugger, R.; Organ, L.; Collier, C.; Atar, D.; Van Eyk, J. Extensive troponin I and T modification detected in serum from patients with acute myocardial infarction. *Circulation* **2000**, *102*, 1221–1226. [CrossRef]
10. Keller, T.; Zeller, T.; Ojeda, F.; Tzikas, S.; Lillpopp, L.; Sinning, C.; Wild, P.; Genth-Zotz, S.; Warnholtz, A.; Giannitsis, E.; et al. Serial changes in highly sensitive troponin I assay and early diagnosis of myocardial infarction. *JAMA* **2011**, *306*, 2684–2693. [CrossRef]
11. Zethelius, B.; Johnston, N.; Venge, P. Troponin I as a predictor of coronary heart disease and mortality in 70-year-old men: A community-based cohort study. *Circulation* **2006**, *113*, 1071–1078. [CrossRef]
12. He, H.; Lowenthal, M.; Cole, K.; Bunk, D.; Wang, L. An immunoprecipitation coupled with fluorescent Western blot analysis for the characterization of a model secondary serum cardiac troponin I reference material. *Clin. Chim. Acta* **2011**, *412*, 107–111. [CrossRef]
13. Apple, F.; Collinson, P. Analytical characteristics of high-sensitivity cardiac troponin assays. *Clin. Chem.* **2012**, *58*, 54–61. [CrossRef] [PubMed]
14. Burklund, A.; Tadimety, A.; Nie, Y.; Hao, N.; Zhang, J.X. Advances in diagnostic microfluidics. *Adv. Clin. Chem.* **2020**, *95*, 1–72. [PubMed]
15. Apple, F.; Pearce, L.; Smith, S.; Kaczmarek, J.; Murakami, M. Role of monitoring changes in sensitive cardiac troponin I assay results for early diagnosis of myocardial infarction and prediction of risk of adverse events. *Clin. Chem.* **2009**, *55*, 930–937. [CrossRef] [PubMed]
16. Li, Y.; Wang, X.; Xu, L.; Wen, X. Rapid identification of falsely elevated serum cardiac troponin I values in a stat laboratory. *Lab. Med.* **2014**, *45*, 82–85. [CrossRef] [PubMed]
17. Ji, X.; Takahashi, R.; Hiura, Y.; Hirokawa, G.; Fukushima, Y.; Iwai, N. Plasma miR-208 as a biomarker of myocardial injury. *Clin. Chem.* **2009**, *55*, 1944–1949. [CrossRef]
18. Guo, J.; Chen, S.; Tian, S.; Liu, K.; Ma, X.; Guo, J. A sensitive and quantitative prognosis of C-reactive protein at picogram level using mesoporous silica encapsulated core-shell up-conversion nanoparticle based lateral flow strip assay. *Talanta* **2021**, *230*, 122335. [CrossRef] [PubMed]
19. Guo, J.; Chen, S.; Tian, S.; Liu, K.; Ni, J.; Zhao, M.; Kang, Y.; Ma, X.; Guo, J. 5G-enabled ultra-sensitive fluorescence sensor for proactive prognosis of COVID-19. *Biosens. Bioelectron.* **2021**, *181*, 113160. [CrossRef]

20. Cho, I.; Paek, E.; Kim, Y.; Kim, J.; Paek, S. Chemiluminometric enzyme-linked immunosorbent assays (ELISA)-on-a-chip biosensor based on cross-flow chromatography. *Anal. Chim. Acta* **2009**, *632*, 247–255. [CrossRef] [PubMed]

21. Imazio, M.; Demichelis, B.; Cecchi, E.; Belli, R.; Ghisio, A.; Bobbio, M.; Trinchero, R. Cardiac troponin I in acute pericarditis. *J. Am. Coll. Cardiol.* **2003**, *42*, 2144–2148. [CrossRef]

22. Wu, W.-Y.; Bian, Z.-P.; Wang, W.; Zhu, J.-J. PDMS gold nanoparticle composite film-based silver enhanced colorimetric detection of cardiac troponin I. *Sens. Actuators B Chem.* **2010**, *147*, 298–303. [CrossRef]

23. Wu, J.; Cropek, D.; West, A.; Banta, S. Development of a troponin I biosensor using a peptide obtained through phage display. *Anal. Chem.* **2010**, *82*, 8235–8243. [CrossRef]

24. Pan, L.; He, M.; Ma, J.; Tang, W.; Gao, G.; He, R.; Su, H.; Cui, D. Phase and size controllable synthesis of NaYbF4 nanocrystals in oleic acid/ionic liquid two-phase system for targeted fluorescent imaging of gastric cancer. *Theranostics* **2013**, *3*, 210. [CrossRef]

25. Chuang, E.-Y.; Huang, W.-H.; Hyo, T.-L.; Wang, P.-C.; Hsiao, Y.-C. IR-inspired visual display/response device fabricated using photothermal liquid crystals for medical and display applications. *Chem. Eng. J.* **2021**, *429*, 132213. [CrossRef]

26. Lu, T.-Y.; Lu, W.-F.; Wang, Y.-H.; Liao, M.-Y.; Wei, Y.; Fan, Y.-J.; Chuang, E.-Y.; Yu, J. Keratin-Based Nanoparticles with Tumor-Targeting and Cascade Catalytic Capabilities for the Combinational Oxidation Phototherapy of Breast Cancer. *ACS Appl. Mater. Interfaces* **2021**, *13*, 38074–38089. [CrossRef]

27. Han, S.; Martin, S. Enantioselective cholesteric liquid crystalline membranes characterized using nonchiral HPLC with circular dichroism detection. *J. Membr. Sci.* **2011**, *367*, 1–6. [CrossRef]

28. Dischinger, S.; Rosenblum, J.; Noble, R.; Gin, D.; Linden, K. Application of a lyotropic liquid crystal nanofiltration membrane for hydraulic fracturing flowback water: Selectivity and implications for treatment. *J. Membr. Sci.* **2017**, *543*, 319–327. [CrossRef]

29. Lu, S.; Guo, Y.; Qi, L.; Hu, Q.; Yu, L. Highly sensitive and label-free detection of catalase by a H2O2-responsive liquid crystal sensing platform. *Sens. Actuators B Chem.* **2021**, *344*, 130279. [CrossRef]

30. Duong, T.; Jang, C.-H. Detection of arginase through the optical behaviour of liquid crystals due to the pH-dependent adsorption of stearic acid at the aqueous/liquid crystal interface. *Sens. Actuators B Chem.* **2021**, *339*, 129906. [CrossRef]

31. Huang, H.; Li, J.; Pan, S.; Wang, H.; Liang, A.; Jiang, Z. A novel small molecular liquid crystal catalytic amplification-nanogold SPR aptamer absorption assay for trace oxytetracycline. *Talanta* **2021**, *233*, 122528. [CrossRef]

32. Su, X.; Huo, W.; Yang, D.; Luan, C.; Xu, J. Label-free liquid crystal immunosensor for detection of HBD-2. *Talanta* **2019**, *203*, 203–209. [CrossRef] [PubMed]

33. Burnouf, T.; Chen, C.-H.; Tan, S.-J.; Tseng, C.-L.; Lu, K.-Y.; Chang, L.-H.; Nyambat, B.; Huang, S.-C.; Jheng, P.-R.; Aditya, R. A bioinspired hyperthermic macrophage-based polypyrrole-polyethylenimine (Ppy-PEI) nanocomplex carrier to prevent and disrupt thrombotic fibrin clots. *Acta Biomater.* **2019**, *96*, 468–479. [CrossRef]

34. Fan, Y.; Chen, F.; Liou, J.; Huang, Y.; Chen, C.; Hong, Z.; Lin, J.; Hsiao, Y. Label-Free Multi-Microfluidic Immunoassays with Liquid Crystals on Polydimethylsiloxane Biosensing Chips. *Polymers* **2020**, *12*, 395. [CrossRef] [PubMed]

35. Chen, F.; Luh, H.; Hsiao, Y. Label-Free, Color-Indicating, Polarizer-Free Dye-Doped Liquid Crystal Microfluidic Polydimethyl-siloxane Biosensing Chips for Detecting Albumin. *Polymers* **2021**, *13*, 2587. [CrossRef] [PubMed]

36. Hsiao, Y.; Tang, C.; Lee, W. Fast-switching bistable cholesteric intensity modulator. *Opt. Express* **2011**, *19*, 9744–9749. [CrossRef]

37. Hsiao, Y.; Wu, C.; Chen, C.; Zyryanov, V.; Lee, W. Electro-optical device based on photonic structure with a dual-frequency cholesteric liquid crystal. *Opt. Lett.* **2011**, *36*, 2632–2634. [CrossRef]

38. Hsiao, Y.; Hou, C.; Zyryanov, V.; Lee, W. Multichannel photonic devices based on tristable polymer-stabilized cholesteric textures. *Opt. Express* **2011**, *19*, 23952–23957. [CrossRef]

39. Hsiao, Y.-C.; Zou, Y.-H.; Timofeev, I.; Zyryanov, V.; Lee, W. Spectral modulation of a bistable liquid-crystal photonic structure by the polarization effect. *Opt. Mater. Express* **2013**, *3*, 821–828. [CrossRef]

40. Hsiao, Y.; Sung, Y.; Lee, M.; Lee, W. Highly sensitive color-indicating and quantitative biosensor based on cholesteric liquid crystal. *Biomed. Opt. Express* **2015**, *6*, 5033–5038. [CrossRef]

41. Luh, H.-T.; Chung, Y.-W.; Cho, P.-Y.; Hsiao, Y.-C. Label-Free Cholesteric Liquid Crystal Biosensing Chips for Heme Oxygenase-1 Detection within Cerebrospinal Fluid as an Effective Outcome Indicator for Spontaneous Subarachnoid Hemorrhage. *Biosensors* **2022**, *12*, 204. [CrossRef]